

TMS orientation and pulse waveform manipulation activates different neural populations: direct evidence from TMS-EEG

Alberto Pisoni^{1,2*}, Alessandra Vergallito¹, Giulia Mattavelli^{1,2}, Erica Varoli³, Matteo Fecchio⁴,
Mario Rosanova^{4,5}, Adenauer G. Casali⁶ and Leonor J. Romero Lauro^{1,2}

¹Department of Psychology, Università degli Studi di Milano-Bicocca, P.za Ateneo Nuovo 1, Milano, Italy

²NeuroMi, Milan center for Neuroscience, Milan, Italy

³Department of Medicine and Surgery, Università degli Studi di Milano-Bicocca, P.za Ateneo Nuovo 1, Milano, Italy

⁴Department of Clinical Sciences, “Luigi Sacco,” Università degli Studi di Milano, Via GB Grassi 74, Milano, Italy

⁵Fondazione Europea di Ricerca Biomedica, FERB Onlus, Milano, Italy

⁶Institute of Science and Technology, Federal University of São Paulo, Rua Talim 330, São José dos Campos, Brazil

*Corresponding author: alberto.pisoni@unimib.it, Department of Psychology, University of Milano-Bicocca, Piazza dell’Ateneo Nuovo, 1, 20126 Milano, Italy.

33 Abstract

34

35 Monophasic and biphasic TMS pulses and coil orientations produce different responses in terms of
36 motor output and sensory perception. Those differences have been attributed to the activation of
37 specific neural populations. However, up to date, direct evidence supporting this hypothesis is still
38 missing since studies were mostly based on indirect measures of cortical activation, i.e., motor evoked
39 potentials or phosphenes. Here, we investigated for the first time the impact of different coil
40 orientations and waveforms on a non-primary cortical area, namely the premotor cortex, by measuring
41 TMS evoked EEG potentials (TEPs). We aimed at determining whether TEPs produced by differently
42 oriented biphasic and monophasic TMS pulses diverge and whether these differences are underpinned
43 by the activation of specific neural populations. To do so, we applied TMS over the right premotor
44 cortex with monophasic or biphasic waveforms oriented perpendicularly (in the anterior-posterior
45 direction and vice-versa) or parallel (latero-medial or medio-laterally) to the target gyrus. EEG was
46 concurrently recorded from 60 electrodes. We analyzed TEPs at the level of EEG sensors and cortical
47 sources both in time and time-frequency domain. Biphasic pulses evoked larger early TEP
48 components, which reflect cortical excitability properties of the underlying cortex, in both parallel
49 directions when compared to the perpendicular conditions. Conversely, monophasic pulses, when
50 oriented perpendicularly to the stimulated gyrus, elicited a greater N100, which is a reliable TEP
51 component linked to GABA_B-mediated inhibitory processes, than when parallel to the gyrus. Our
52 results provide direct evidence supporting the hypothesis that TMS pulse waveform and TMS coil
53 orientations affect which neural population is engaged.

54

55

56

57

58

59

60

61 Keywords: TMS-EEG, TMS, coil orientation, waveform, biphasic, monophasic, TEP

62

63 Introduction

64

65 Despite its large use for research and clinical purposes, different issues on the effects of Transcranial
66 Magnetic Stimulation (TMS) on the cerebral cortex are still unknown (Triesch et al., 2015). One
67 interesting methodological aspect concerns the differences in neurophysiological responses evoked
68 by monophasic and biphasic stimulation pulses. In the monophasic mode, a strong initial current flow
69 is followed by a smaller current in the opposite direction. The initial flow has a quick peak (about 50
70 μ s after pulse onset) and effectively excites neurons, while the subsequent return current, which lasts
71 several hundreds of μ s, does not elicit action potentials (Groppa et al., 2012). The biphasic pulse,
72 instead, has a cosine waveform: an initial peak is followed by a reversal current and by another
73 subsequent peak. In this pulse configuration, each phase of the pulse induces an effective stimulation,
74 which spreads in the same or opposite direction as the initial one. In the biphasic mode, then, all pulse
75 phases are effective in stimulating the cortical nervous tissue but seem to involve different neuronal
76 populations (Groppa et al., 2012), even if the second half cycle is more effective.

77 It has been reported that these two TMS pulse waveforms induce differential electrophysiological
78 outputs as measured by Motor Evoked Potentials (MEPs; e.g., Kammer et al., 2001; Niehaus et al.,
79 2000; Sommer et al., 2006) and can induce distinct plastic after-effects following repetitive TMS
80 protocols (Pascual-Leone et al., 1994; Sommer et al., 2002; Tings et al., 2005). The comparison
81 between single monophasic and biphasic pulses over the motor cortex (M1) suggests that at a given
82 amplitude of the initial current, biphasic stimulation is more effective than the monophasic one in
83 eliciting MEPs (Kammer et al., 2001). For rTMS, the effect of the two pulse configurations seems to
84 be reversed. Reports, indeed, showed that the inhibition of M1 excitability exerted by monophasic
85 low-frequency rTMS (1HZ-rTMS) is more prolonged compared to the biphasic one (Sommer et al.,
86 2002; Taylor & Loo, 2007), especially when the current is oriented in the anterior-posterior direction
87 (Tings et al., 2005). Conversely, monophasic posterior-anterior rTMS induces an increase of M1
88 cortical excitability as, to a lesser extent, also did the latero-medial orientation (Tings et al., 2005).
89 Similar results were also obtained over primary visual cortex (V1), where low-frequency monophasic
90 rTMS decreased contrast sensitivity for visual stimuli after stimulation (Antal et al., 2002). Some
91 authors suggested that monophasic rTMS activates a relatively uniform neural population and could
92 therefore be more effective in producing sustained plastic after-effects. Conversely, biphasic pulses
93 generate a more complex pattern of neural activations (Arai et al., 2005, 2007; Sommer et al., 2002),
94 reducing the overall stimulation-induced after-effects. The ultimate reason for these differences,
95 however, is still debated (Sommer et al., 2006) and so is the role of the different components of
96 biphasic pulses for in vivo and in vitro studies (Kammer et al., 2001; Maccabee et al., 1998). Another

97 compelling issue is the orientation of the TMS-induced electric field, which indeed has been
98 associated with different neurophysiological responses, due to dissimilar activations of the underlying
99 neural population or by recruiting different neurons (for a review see Di Lazzaro et al., 2008).
100 Crucially, research focused on the neurophysiological changes occurring in M1, since motor cortex
101 activation can be indirectly recorded via MEPs or cortico-spinal recordings, or in V1, by analyzing
102 phosphenes perception. However, TMS protocols are widely used in research (see Luber & Lisanby,
103 2014 for a review) and clinical protocols (see Lefaucheur et al., 2014 for a review) in a variety of
104 areas, which have very different cytoarchitectonic and neurophysiological properties and cannot be
105 directly compared with M1 or V1 (Taylor & Loo, 2007). A further element preventing a clear
106 understanding of the processes underlying different TMS protocols is that studies often report coil
107 orientation referred to the subjects' head, only inferring the underlying cortical geometry. For
108 example, the 45° angle usually applied for an optimal M1 stimulation, is reported to be perpendicular
109 to the precentral gyrus, but a vast number of studies do not have individual MRIs to check if this is
110 true (Sparing et al., 2010).

111 Improving our knowledge of TMS mechanisms can be useful to optimize research and treatment
112 protocols. In this perspective, we used a navigated TMS combined with electroencephalography
113 (TMS-EEG) system to investigate the impact of TMS pulse waveform and coil orientation on cortical
114 excitability. Specifically, we compared monophasic and biphasic pulses delivered over the right
115 premotor cortex orienting the coil perpendicularly (i.e. applying an anterior-posterior pulse, A – P, or
116 posterior-anterior one, P – A) or parallel (i.e. applying a latero-medial, L – M, or medio-lateral, M –
117 L, pulse) to the right premotor cortex, localized on individual MRIs. The main advantage of TMS-
118 EEG approach is to provide real-time and direct information on cortical reactivity through TMS-
119 evoked potentials (TEPs) recording. TEPs have been indeed consistently reported as being an
120 informative measure of cortical excitability (Casarotto et al., 2010; Ilmoniemi et al., 1997; Ilmoniemi
121 & Kičić, 2010; Lioumis et al., 2009) and connectivity (Komssi et al., 2002, 2004, 2007; Massimini
122 et al., 2005; Mattavelli et al., 2013, 2016; Pisoni et al., 2017; Romero Lauro et al., 2014, 2016).
123 Interestingly, previous research linked TEPs components with specific neurophysiological properties
124 of the stimulated cortical area. In particular, early TEP components (0-60ms) have been described as
125 reflecting different processes: on one hand, ipsilateral components reflected excitability properties of
126 the targeted region, being affected by neurophysiological interventions aimed at modulating synaptic
127 strength and cortical excitability such as tDCS (Pellicciari et al., 2013; Pisoni et al., 2017) or rTMS
128 (Esser et al., 2006; Veniero et al., 2010, 2012); conversely, a component peaking at ~45ms and
129 centered on contralateral homologue areas seems to be involved in GABA_A mediated intracortical
130 inhibition (Premoli et al., 2014; Ziemann et al., 2015). Expressly for the premotor cortex, one of the

131 most consistently described components peaks around 100 ms from TMS pulse, and is related to
132 GABA_B cortico-cortical inhibition (Ilmoniemi & Kičić, 2010; Kičić et al., 2008; Premoli et al., 2014).
133 By systematically varying TMS pulse waveform, orientation, and direction we thus aimed at
134 investigating possible differences in TEPs components and amplitude to assess which
135 neurophysiological responses are triggered by different stimulation protocols and to measure their
136 efficacy in eliciting cortical responses.

137

138 Material and Methods

139 *Participants*

140 Ten healthy, right-handed volunteers (6 male, mean age 28.3, SD 6.4, range 21-39) participated in
141 the study. Each participant completed an Adult Safety Screening Questionnaire (Keel et al., 2001)
142 and gave informed written consent before study procedures. Participants with any contraindication,
143 such as brain injury or surgery, heart attack or stroke and use of medications known to alter cortical
144 excitability (e.g., anti-depressant medication), were excluded (Rossi et al., 2009). Each subject had
145 an individual structural MRI of the brain to be used for neuronavigation. The study was performed in
146 the TMS-EEG laboratory of the University of Milano-Bicocca and was approved by the local Ethic
147 Committee.

148

149 *Procedure*

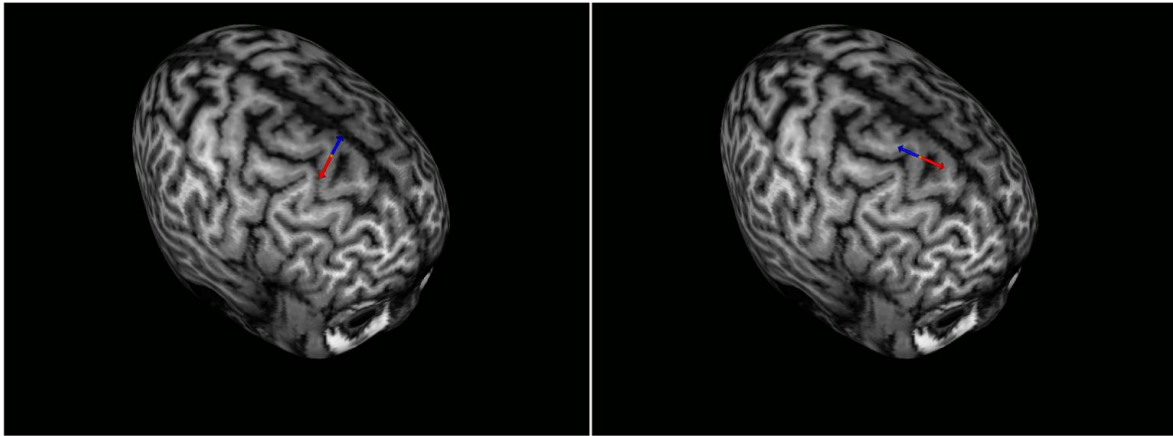
150 Each participant took part in two experimental sessions separated by ~6 months between them, each
151 consisting of four TMS-EEG recordings performed with different TMS parameters, all delivered over
152 the right premotor cortex (Fig.1a), varying for both TMS waveform (monophasic vs biphasic),
153 orientation over the target gyrus (parallel vs perpendicular), and direction (A - P and P - A for the
154 perpendicular orientation and M - L and L - M for the parallel orientation). Each recording lasted
155 about seven mins, during which participants fixated a white cross in black screen (17") in front of
156 them. Around 180 TEPs were recorded in each condition that, as previously reported, allows having
157 a good number of artefact-free trials for analysis (Casarotto et al., 2010; Pisoni et al., 2017; Romero
158 Lauro et al., 2014). The order of the eight TMS conditions was quasi counterbalanced across subjects,
159 meaning that waveforms and orientations were counterbalanced, while the A - P and L - M directions
160 were always performed in session 1 and P - A and M - L directions in session 2.

161

162 *TMS stimulation*

163 TMS was delivered using an Eximia™ TMS stimulator (Nexstim™, Helsinki, Finland) using one
164 monophasic and one biphasic focal figure of eight 70-mm coils. The stimulation target was the right

165 premotor area. High-resolution (1x1x1 mm) structural magnetic resonance images (MRI) were
166 acquired for each participant using a 3 T Intera Philips body scanner (Philips Medical Systems, Best,
167 NL). TMS target was identified on individual MRIs using an integrated Navigated Brain Stimulation
168 (NBS) system (Nexstim™, Helsinki, Finland) which employs infrared-based frameless stereotaxy, to
169 map the position of the coil and the participant's head, within the reference space of the individual's
170 MRI space. The NBS system allowed to continuously monitor the position and orientation of the coil,
171 thus assuring precision and reproducibility of the stimulation across recordings. The importance of
172 using NBS with individualized MRIs rather than adjusting the coil angle and position according to
173 scalp landmarks is crucial to correctly target the desired cortical area, which may be differently
174 displaced in each subject (Sparing et al., 2010). No individual functional MRI was acquired, thus the
175 functional specificity of the stimulation area could not be assessed. The NBS system estimated on-
176 line the intensity (V/m) of the intracranial electric field induced by TMS at the stimulation hotspot,
177 accounting for the head and brain shape of each participant, and taking into consideration the distance
178 from scalp and coil position. Resting Motor Threshold, indeed, could have been a misleading measure
179 to calibrate stimulation intensity, since the cortical thickness and cortical reactivity may greatly vary
180 between M1 and the premotor cortex (e.g., see Kähkönen et al., 2005; Peterchev et al., 2012). We
181 thus calibrated TMS intensity considering the estimated induced cortical electric field and checking,
182 in a short preliminary recording before each real session, whether an on-line response of at least ~ 2
183 μ V could be evoked, by starting at an estimated intensity of the electrical induced field of 90 V/m.
184 Mean estimated electric field at the stimulation target for all condition are reported in Tab. 3.
185 Critically, mean estimated induced electric field did not differ between any of the stimulation
186 protocols (all $p > .14$). The corresponding mean stimulation intensities, expressed as a percentage of
187 the maximal output of the stimulator, are reported in Tab. 4. Crucially, within monophasic and
188 biphasic conditions, mean stimulator output did not differ between the four different directions (all
189 $p > .08$). The coil was tangentially placed to the scalp, and adjusted for each participant to direct the
190 electric field parallel (L - M or M - L) or perpendicular (A - P or P - A) to the shape of the cortical
191 gyrus (See Fig.1). The stimulation direction is relative to the first and unique cycle of the monophasic
192 and the second, strongest cycle of the biphasic pulse. As in previous studies (Julkunen et al., 2008;
193 Mütanen et al., 2013; Zanon et al., 2013), the stimulation of the premotor cortex did not evoke evident
194 facial muscular artefacts, and no twitch of the contralateral upper limbs were indeed reported for any
195 subject. TMS pulses were delivered at an inter-stimulus interval randomly jittering between 2000 and
196 2300 ms.



197

198

199

200

201

202 *EEG Recording during TMS*

203

204

205

206

207

208

209

210

211

212

213

214

215

216

217

218

219

220

221

222

Fig. 1: NBS screenshots displaying stimulation position and direction in the parallel (M – L, left) and perpendicular (P – A, right) orientations. The red arrow indicates the direction of the strongest phase of the stimulation (i.e., the only one in the monophasic and the second one of the biphasic pulse).

EEG signal was continuously recorded using a TMS compatible 60-channels amplifier (Nexstim Ltd., Helsinki, Finland), which prevents saturation using a proprietary sample-and-hold circuit which holds the amplifier output constant from 100 μ s pre to 2 ms post-TMS pulse (Virtanen et al., 1999). Two extra-electrodes placed over the forehead were used as ground. Eye movements were recorded using two additional electrodes placed near the eyes to monitor ocular artefacts. As in previous studies, during EEG recordings, participants wore earplugs and heard a continuous masking noise to cover TMS coil discharge (Casarotto et al., 2010; Massimini et al., 2005; Romero Lauro et al., 2014), avoiding thus the emergence of auditory evoked potentials (Ter Braack et al., 2015). Electrodes impedance was kept below five k Ω , and EEG signals were recorded with a sampling rate of 1450 Hz and in common reference.

Data pre-processing was carried out using Matlab R2012a (Mathworks, Natick, MA, USA). EEG recordings were band-pass filtered between 1 and 45 Hz. Then, EEG signals were split into epochs starting 800 ms before and ending 800 ms after the pulse. EEG signals were down-sampled to 725 Hz. Trials with excessive artefacts were removed by a semi-automatic procedure and visual inspection (Casali et al., 2010) and TEPs were computed by averaging selected artefact-free single epochs. Bad channels were interpolated using spherical interpolation function of EEGLAB (Delorme & Makeig, 2004). TEPs were then averaged-referenced and baseline corrected between -300 and -50 ms before the TMS pulse. Independent component analysis (ICA) was applied to remove residual artefacts (Delorme et al., 2007). The average number of accepted trials considered in the analysis is reported in supplementary Tab. 1 of the Supplementary Materials while the mean signal to noise ratio,

223 which was greater than 1.55 in all sessions (Casali et al., 2013), is reported in Tab. 2 of the
224 Supplementary Materials.

225 To assess where and when cortical responses to TMS differed within pulse waveform according to
226 coil orientation, TEPs were rectified and compared through a cluster-based test (Maris & Oostenveld,
227 2007) as implemented in the FieldTrip MATLAB toolbox for M/EEG analysis (freely available at
228 <http://fieldtrip.fcdonders.nl/>; Oostenveld et al., 2011). Specifically, a whole-head, cluster-based
229 permutation-corrected t-test was run between A – P, P – A, M – L, and L – M orientations within
230 each coil type. To assess differences in amplitude, this procedure performs 10000 permutations by
231 shuffling trial labels. Then, for each permutation, independent sample t-tests are performed at each
232 time-point. All samples with a statistic corresponding to a P-value smaller than .05 are clustered
233 together by spatial proximity. Finally, the cluster statistic is computed by taking the sum of the t-
234 values within each cluster. The cluster-corrected threshold is then obtained by computing the
235 permutation distribution of the maximum cluster statistic. This procedure thus corrects for multiple
236 comparisons by permuting the data and clustering them based on their spatial and temporal proximity.
237 In our case, for each comparison, permutations were performed for the whole 0-250ms time window
238 with a permutation-significant level of $p=.05$. Critically six comparisons were performed within each
239 waveform: A – P vs. P – A; M – L vs. L – M; A – P vs. M – L; A – P vs. L – M; P – A vs. L – M; P
240 – A vs. M – L.

241 To better refine where the cortical activation induced by the different TMS protocols was taking
242 place, source analysis was performed. Firstly, individual standardized meshes were reconstructed for
243 each participant, starting from their structural MRIs (SPM8, Ashburner et al., 2011; Litvak et al.,
244 2011), obtaining meshes of cortex, skull and scalp compartments (containing 3004, 2000 and 2000
245 vertices, respectively), normalized to the Montreal Neurological Institute (MNI) atlas (Casali et al.,
246 2010). Then, for each participant, EEG sensor position was aligned to the canonical anatomical
247 markers (pre-auricular points and nasion), and the forward model was computed. The inverse solution
248 was computed on the average of all artefact-free TMS-EEG trials using the weighted minimum norm
249 estimate with smoothness prior, following the same procedures as in Casali et al. (2010). This method
250 is advantageous because it provides stable solution also in the presence of noise (Silva et al., 2004),
251 and does not require any a priori assumption about the nature of the source distribution (Hämäläinen
252 & Ilmoniemi, 1994). After source reconstruction, a statistical threshold was computed to assess when
253 and where the post-TMS cortical response differed from pre-TMS activity (i.e., to identify TMS-
254 evoked response). To do so, a nonparametric permutation-based procedure was applied (Pantazis et
255 al., 2003). Binary spatial-temporal distribution of statistically significant sources was obtained, and
256 thus only information from significant cortical sources was used for further analyses. As a measure

257 of global cortical activation, we cumulated the absolute Significant Current Density (global SCD,
258 measured in mA/mm², Casali et al., 2010) over all 3004 cortical vertexes and over three time
259 windows encompassing the TEPs components under investigation (0-30 ms, 30-80 ms and 80-130
260 ms) for each TMS protocol. Moreover, a local SCD in the vertexes within the BA targeted by TMS,
261 i.e., right BA 6 identified using an automatic tool of anatomical classification (WFUPickAtlas tool;
262 <http://www.ansir.wfubmc.edu>), was computed. Finally, an index of current scattering (SCS, Casali et
263 al., 2010) was computed to estimate how spread the induced signal was. These measures were
264 compared between stimulation protocols, within each coil type, using a series of linear mixed models
265 (Baayen et al., 2008) in R computing environment (R Development Core Team, 2008). Indices
266 derived from the source modeling were included in the model as dependent variables, while the
267 stimulation protocol inclusion as fixed effect was estimated with an LRT procedure (Baayen et al.,
268 2008), including it in the final model only if it significantly increased the model's goodness of fit.
269 The by-subject random slope was included as random factor.

270 Finally, to investigate whether the TMS evoked responses differed not only in amplitude, but also in
271 spectral components, a time-frequency analysis was run. In particular, within Fieldtrip toolbox, the
272 TMS induced time-frequency representations (TFR) of power was computed by convolving single
273 trials with Morlet wavelets that had a width of 3.5 cycles (see Rosanova et al., 2009 for a similar
274 procedure). Wavelet convolution was done between 2 and 40 Hz, in 2 Hz steps, and a time step of
275 2ms between -800ms and +800ms around the TMS pulse. To assess the significance of differences in
276 oscillation power across conditions, the same procedure adopted for the source analyses data was
277 used. In particular, mean power values mediated from the 4 electrodes near the TMS coil (Fz, F2,
278 FCz, FC2) were computed for 4 different frequency bands (θ : 4-7 Hz; α : 8-12 Hz; β : 13-30 Hz; high
279 β : 31-40 Hz), were baseline normalized, and finally were cumulated over the whole TEP time window
280 (0-250ms). These values were used for the linear mixed regression previously described, comparing
281 the four monophasic and the four biphasic directions separately.

282

283 Results

284

285 Effects of coil orientation on TEPs evoked by monophasic pulses

286

287 Amplitude at the scalp level

288

289 To specifically assess which part of the evoked cortical response differed according to coil
290 orientation, the amplitude of the evoked response was compared with a cluster based permutation t-
291 test on the whole 0-250ms TEP duration.

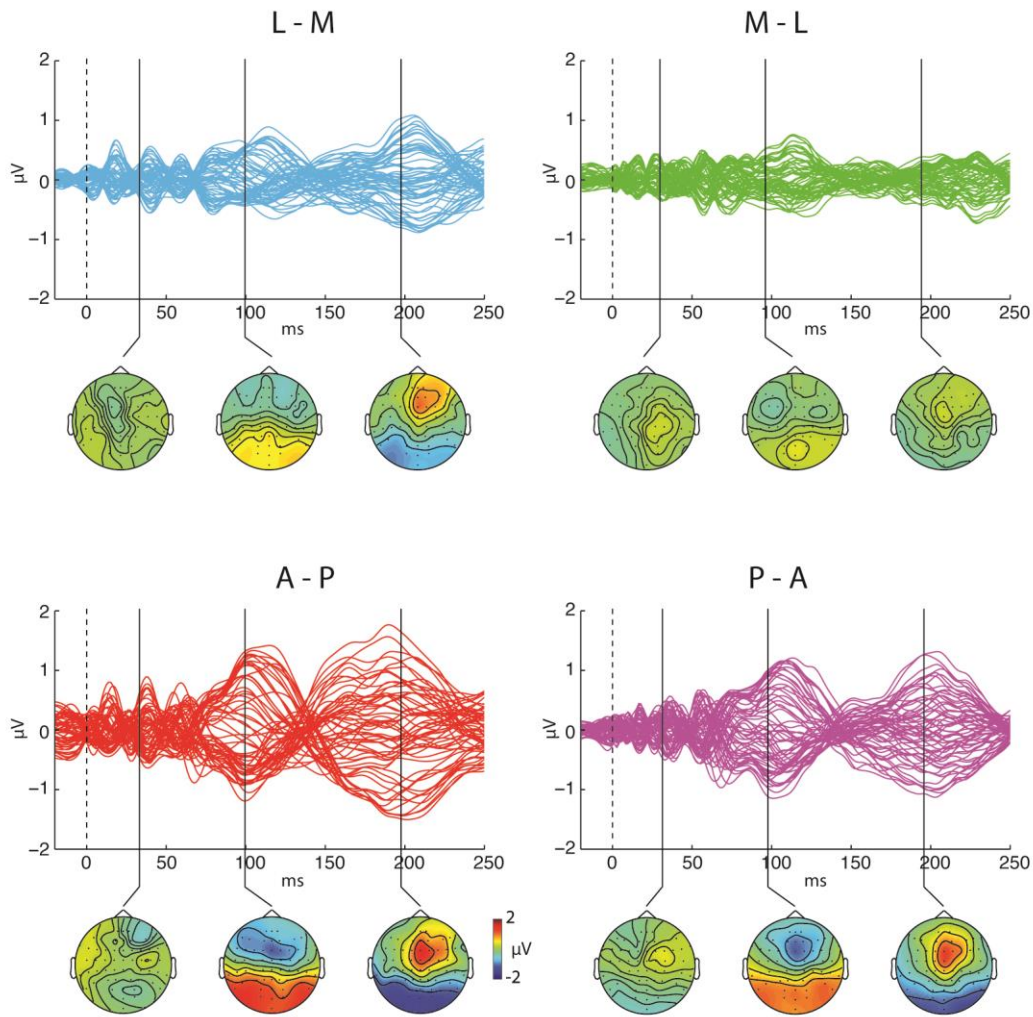
292 Fig. 2 shows the unrectified grand average of TEPs in the four monophasic conditions. As the first
293 components, with a latency comprised within the first 70ms, have a similar time-course and amplitude
294 in all orientations and directions, responses start to differ in the component peaking around 100ms,
295 where the perpendicular orientations, in both A - P and P - A directions, elicit a greater response as
296 compared to the parallel orientations, similarly in the M - L and L - M directions. The following late
297 component, peaking around 200 ms, seems greater for the A-P orientation, even if a consistent
298 response is also recorded for the L-M direction.

299 The cluster-based analysis confirmed these observations. No significant differences were present for
300 any components between the two directions within parallel and perpendicular orientations. By
301 contrast, when comparing the two orientations, A - P stimulation resulted in a greater 100ms
302 component when delivering L - M (significant cluster from 80 to 130ms, $p < .001$) and M - L
303 monophasic TMS (significant cluster from 50 to 160ms, $p < .001$). Moreover, this latter comparison
304 showed that A - P stimulation triggered greater components in a significant early cluster between 170
305 and 240ms ($p = .014$) and an earlier one, between 20 and 40ms ($p = .038$). The topography of these
306 differences, centred around 100ms post TMS (Fig. 3), shows higher evoked activity in the
307 perpendicular A - P direction over a large cluster of electrodes, comprising a set of sensors located
308 in the fronto-central areas, including the region under the TMS coil and its contralateral homologue
309 when compared to both the parallel L - M and M - L directions.

310 Similarly, P - A monophasic TMS elicited greater 100ms component compared to both L - M
311 (significant cluster 90-110ms, $p = .05$) and M - L (significant cluster 80-130ms, $p = .006$) directions
312 (see Fig. 3).

313

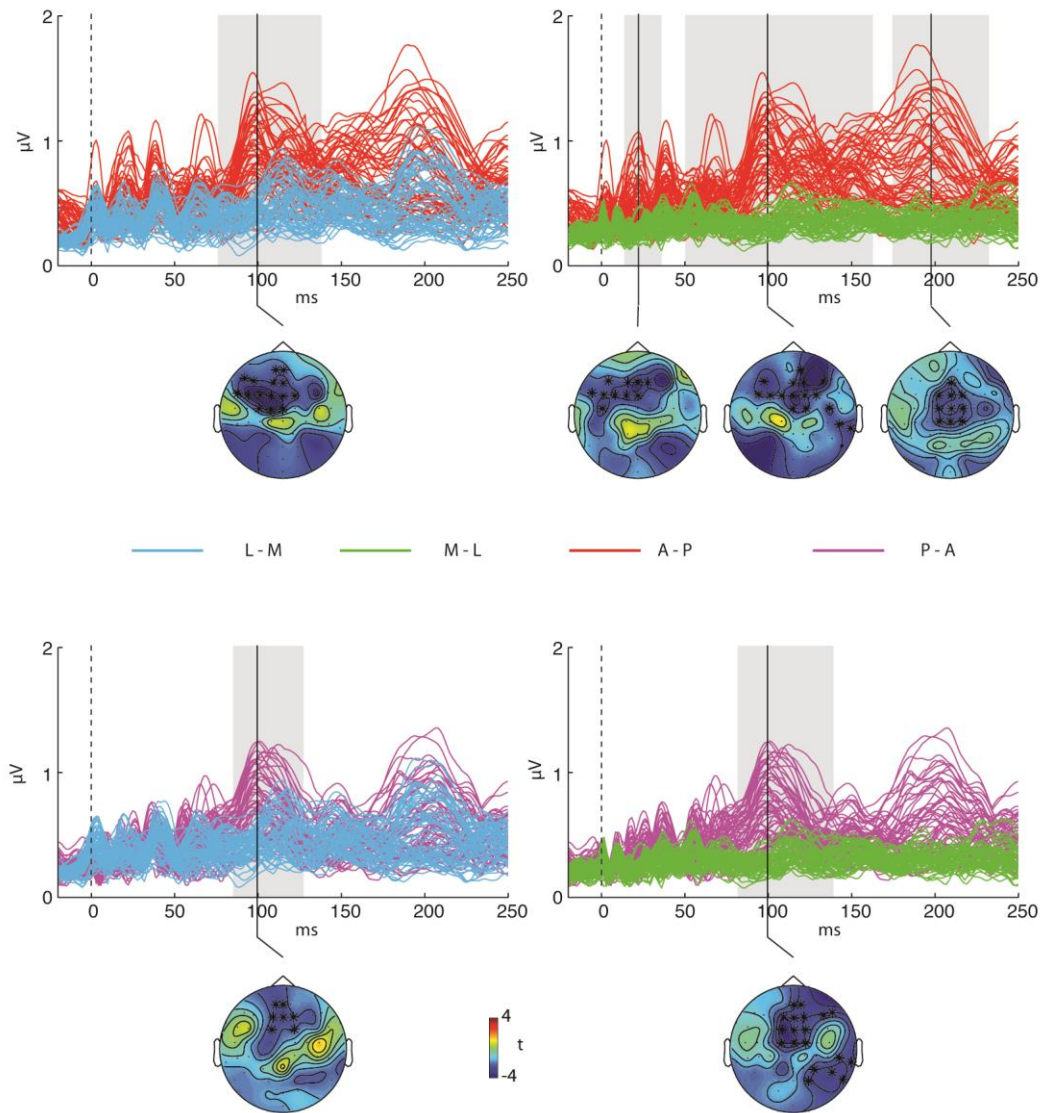
Monophasic



314

315 *Fig. 2: Butterfly plots and scalp topographies of TEPs grand average triggered by monophasic TMS. Top line shows*
316 *results for the L – M and M – L directions while bottom line shows results for the A – P and P – A directions.*

317



318
 319 *Fig. 3: Results of the cluster based analysis for the monophasic pulse waveform. Top line displays a superimposition of*
 320 *rectified TEPs for the L – M and A – P (left) and M – L and A – P conditions (right). Grey shaded areas represent time*
 321 *windows in which the two waveforms statistically differ. Scalp topographies represent the distribution of the statistics for*
 322 *each comparison with significant electrodes plotted in bold. The same is reported in the bottom line for the comparison*
 323 *between P – A and L – M (left) and M – L (right) protocols.*

324

325 Cortical Source modeling

326

327 Confirming the results at the sensors level, global SCD was smaller in the late component (80-130ms)
 328 for the L – M protocol compared to both A – P ($\chi^2(1) = 6.61$; $p = .01$) and P – A ($\chi^2(1) = 5.25$; $p = .02$)
 329 perpendicular orientations. M – L protocol, instead, showed marginal differences with the A – P and
 330 P – A directions ($\chi^2(1) = 3.4$; $p = .06$ and $\chi^2(1) = 3.3$; $p = .06$ respectively; see Fig. 4). Local SCD,
 331 computed in BA6, which was targeted by TMS, showed a clear increase in the induced current in the
 332 100ms component for the perpendicular orientations compared to the parallel ones. In particular, A –

333 P protocol elicited a greater late component compared to both L – M ($\chi^2(1)= 4.81$; $p=.028$) and M –
334 L ($\chi^2(1)= 5.49$; $p=.019$) parallel directions. Similarly, the P – A stimulation induced a greater 100ms
335 component compared to the L – M ($\chi^2(1)= 5.44$; $p=.02$) and M – L ($\chi^2(1)= 7.63$; $p=.005$) protocols
336 (See Fig. 4). No other significant difference was present for the early components.

337 The Significant Current Scattering confirmed that, while in the first and second time-windows no
338 difference in the spread of the induced current was present between the four protocols, in the third
339 time window current spreads more over the cortex in the perpendicular compared to the parallel
340 orientations. In particular, in the A – P direction SCS was greater compared to both L – M ($\chi^2(1)=$
341 5.6 ; $p=.017$) and M – L ($\chi^2(1)= 3.9$; $p=.049$) conditions. Similarly, the P – A protocol induced more
342 spread cortical activity compared to the L – M condition ($\chi^2(1)=5$; $p=.025$) and marginally compared
343 to the M – L one ($\chi^2(1)= 3.6$, $p=.056$). In the first time-window, instead, the A – P protocol induced
344 more widespread activity compared to the P – A direction.

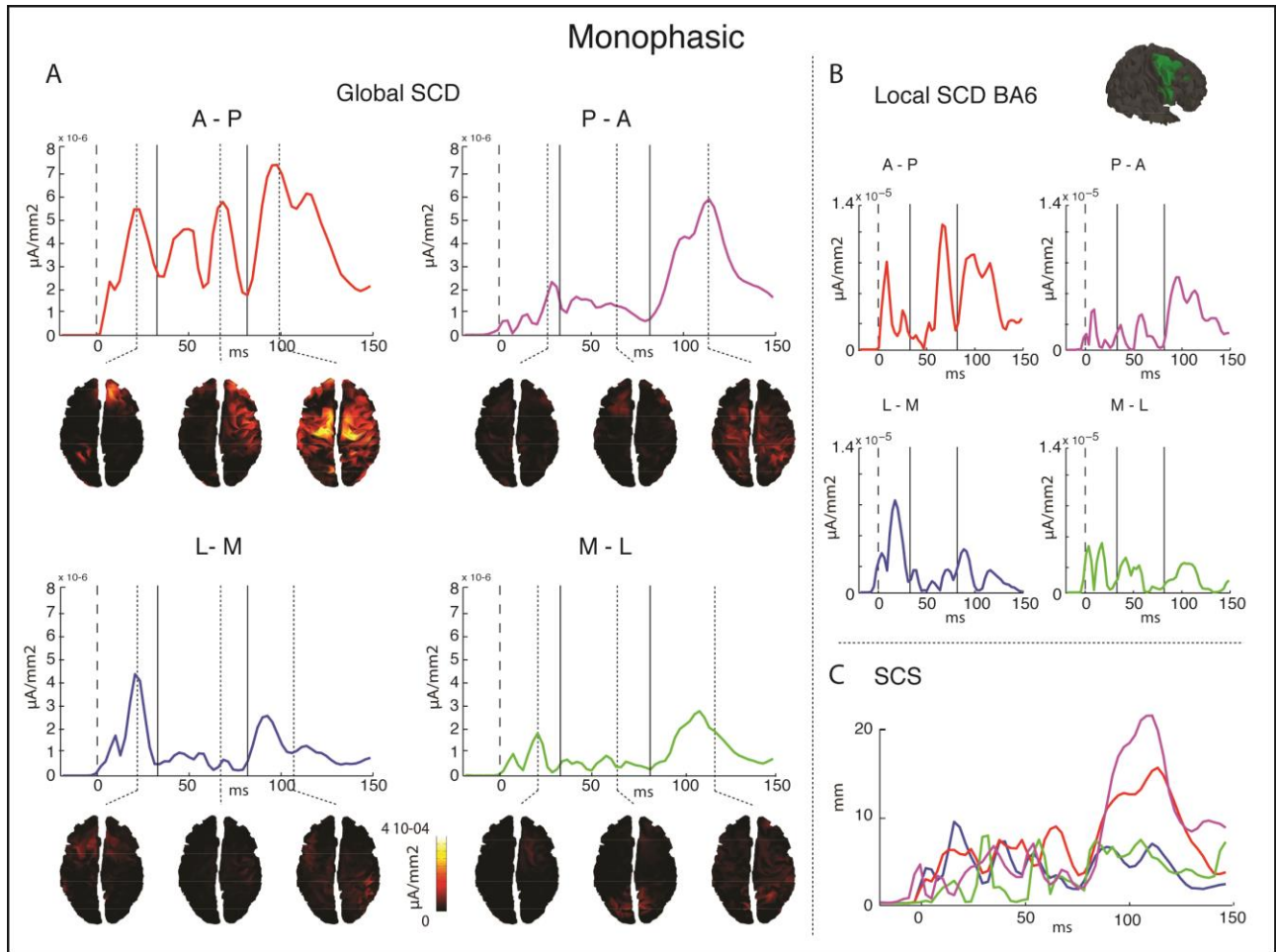
345

346 Time-Frequency analysis

347

348 Time-Frequency analysis showed a different effect of TMS orientation and direction on the
349 oscillatory cortical response. A – P stimulation induced greater oscillation in the theta, alpha, beta
350 and high beta bands compared to both L – M (θ : $p<.001$; α : $p<.001$; β : $p<.001$; high β : $p=.013$) and
351 M – L (θ : $p=.02$; α : $p=.046$; β : $p=.018$ high β : $p<.001$) parallel directions. Conversely, P – A
352 perpendicular stimulation elicited greater activity in all the considered frequency bands compared
353 only to the L – M direction (θ : $p=.029$; α : $p=.046$; β : $p=.05$). Perpendicular stimulation differed in the
354 alpha, beta and high beta bands, with A – P direction eliciting greater power in both frequency bands
355 compared to P – A direction (α : $p=.024$; β : $p=.001$; high β : $p=.015$). Conversely, parallel directions
356 differed in the alpha ($p=.025$) and beta ($p=.007$) bands, with a higher power in the L – M compared
357 to the M – L direction (see Fig 5).

358



359

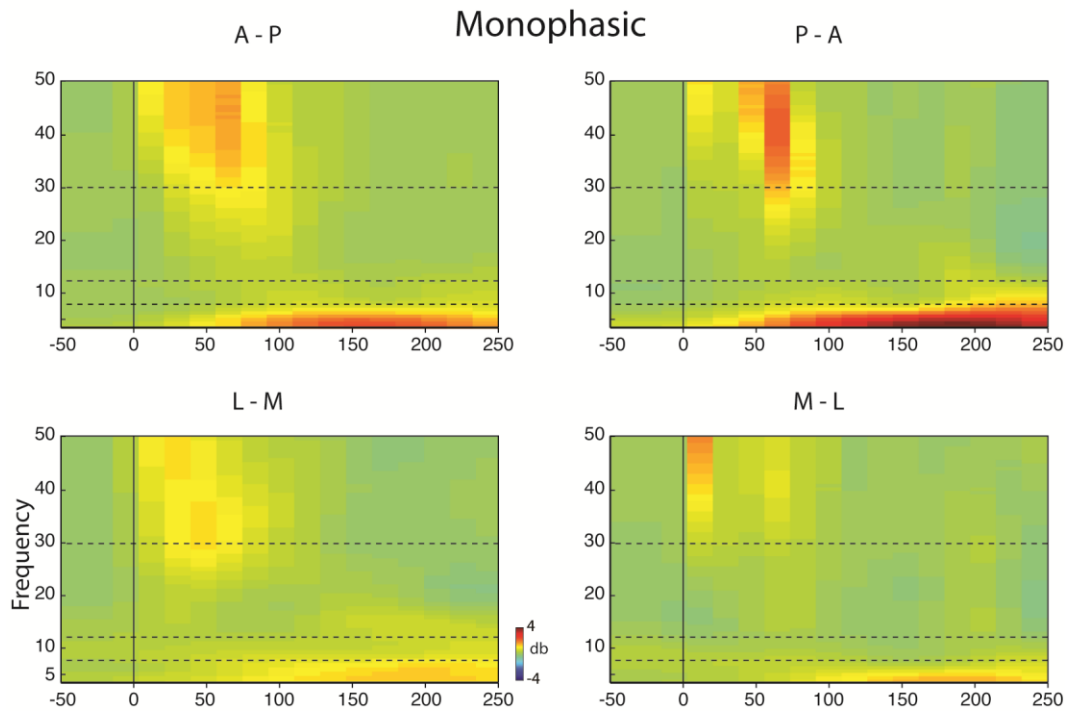
360

361

362

363

Fig. 4: Results of the source analyses for the monophasic protocols. A) plot of the global SCD for the four directions with cortical source reconstruction at the local maxima for each of the three analyzed time windows (0-30ms; 30-80ms; 80-150ms). B) Plot of local SCD in the right BA6. C) plot of the SCS for the 4 protocols.



364

365

366

367

368

369 Effects of coil orientation on TEPs evoked by biphasic pulses

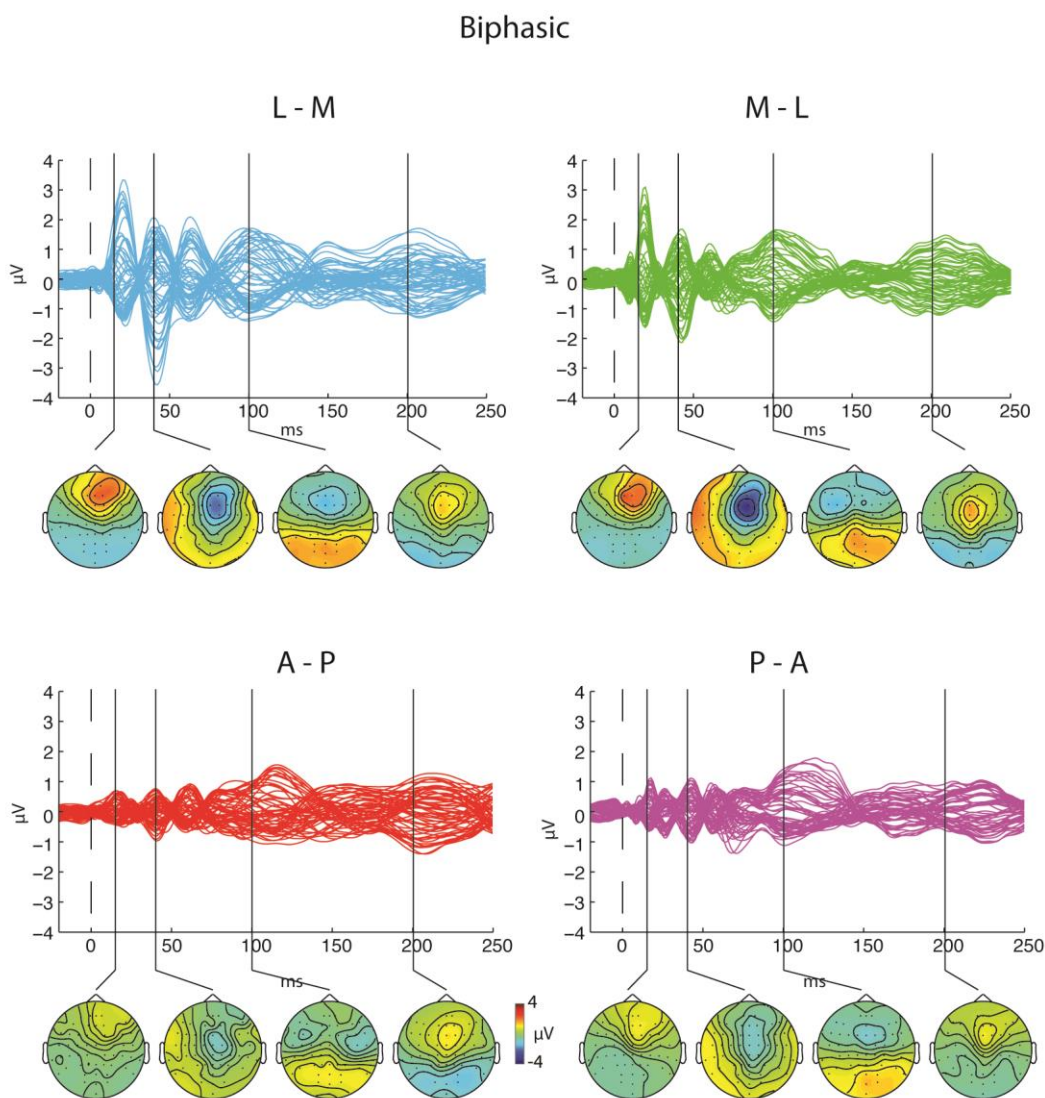
370

371 Amplitude at the scalp level

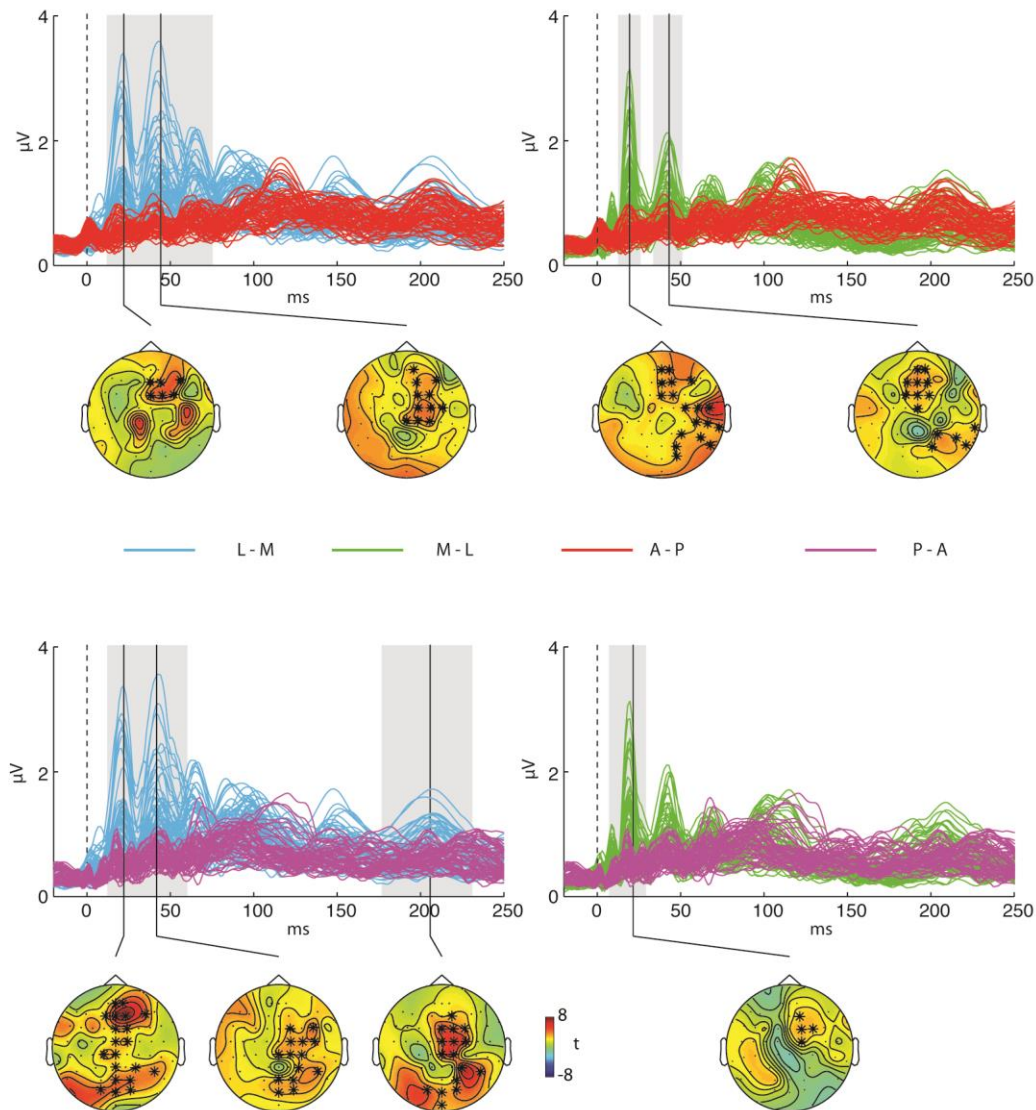
372

373 Fig. 6 shows the unrectified grand average of TEPs in the four biphasic conditions. For this pulse
374 waveform, responses in the two orientations differ in the very early components, lasting from 15 ms
375 to 70 ms post-TMS onset. In this case, the parallel orientations, in both the L – M and M – L directions,
376 elicits greater TEPs components. The cluster-based analysis confirmed that by delivering biphasic
377 stimulation parallel to the gyrus, the earlier components resulted greater as compared to the
378 perpendicular one. In particular, the M – L direction triggered a greater component peaking around
379 15 ms post-TMS compared to both A – P (significant cluster from 10 to 20ms, $p=.01$) and P – A
380 conditions (significant cluster from 10 to 30 ms, $p=.01$). Moreover, the M – L component arising
381 around 40ms post-TMS was greater than the same component in the A – P condition (significant
382 cluster from 30 to 50ms, $p=.04$). The scalp distribution of the significant differences between M – L,
383 and P – A and A – P protocols show central frontal greater amplitude for the parallel compared to the
384 two perpendicular directions. Similarly, the L – M direction induced a greater early TEP component
385 than the perpendicular biphasic condition in both the A – P (significant cluster from 10 to 70 ms,

386 $p < .001$) and P – A (significant cluster from 10 to 20 ms, $p = .02$; from 30 to 60 ms, $p = .016$) directions.
387 Also, these differences are distributed around frontocentral electrodes (See Fig. 7). Moreover, L – M
388 condition elicited a greater late component when compared to the perpendicular P – A (significant
389 cluster from 180 to 210ms, $p = .009$) and parallel M – L (significant cluster from 150 to 180ms, $p = .028$)
390 protocols. This difference between the parallel orientations with biphasic pulses has a topography
391 encompassing frontal and parietal left electrodes, thus contralateral with respect to the TMS hotspot
392 (see Fig.7).
393



394
395 *Fig. 6: Butterfly plots and scalp topographies of TEPs grand average triggered by biphasic TMS. Top line shows results*
396 *for the L – M and M – L directions while bottom line shows results for the A – P and P – A directions.*
397



398

399 *Fig. 7: Results of the cluster based analysis for the biphasic pulse waveform. Top line displays a superimposition of*
 400 *rectified TEPs for the L – M and A – P (left) and M – L and A – P (right) conditions. Grey shaded areas represent time*
 401 *windows in which the two waveforms statistically differ. Scalp topographies represent the distribution of the statistics for*
 402 *each comparison with significant electrodes plotted in bold. The same is reported in the bottom line for the comparison*
 403 *between P – A and L – M (left) and M – L (right) protocols.*

404

405

406

407 **Cortical Source modeling**

408

409 Global SCD was greater for the early time window in both parallel directions compared to the
 410 perpendicular ones (L – M vs: A – P $\chi^2(1) = 11.7$; $p < .001$; P – A $\chi^2(1) = 15.8$; $p < .001$; M – L vs: A –
 411 P $\chi^2(1) = 3.6$; $p = .05$; P – A $\chi^2(1) = 6.8$; $p = .009$). This greater induced cortical current in the parallel
 412 orientation was still present in the second time window (30-80ms) for the L – M direction compared

413 to both A – P ($\chi^2(1)=5.1$; $p=.024$) and P – A ($\chi^2(1)=6.2$; $p=.012$) directions, and for the M – L
414 condition compared to the P – A direction ($\chi^2(1)=14.3$; $p<.001$). Greater late activity was also present
415 for the L – M stimulation compared to the A – P one ($\chi^2(1)=6.2$; $p=.013$). No difference in SCD was
416 present within the two parallel or perpendicular orientations. In the cortical region near the TMS
417 target, namely right BA6, local SCD followed a similar pattern to global SCD, yet reduced in time-
418 course. In particular, in the first time-window, L – M orientation showed a greater induced current
419 compared to the A – P ($\chi^2(1)=11.6$; $p<.001$) and the P – A ($\chi^2(1)=13.2$; $p<.001$) protocols, as did the
420 M – L condition (A – P $\chi^2(1)=3.8$; $p=.05$; P – A $\chi^2(1)=5.04$; $p=.025$). In the second time-window,
421 instead, only the L – M protocol induced greater activity compared to the A – P condition ($\chi^2(1)=5.2$;
422 $p=.022$). No other difference resulted significant (See Fig. 8).

423 SCS computation showed that in the first time window, current was more widespread in the L – M
424 condition compared to both the A – P ($\chi^2(1)=4.36$; $p=.037$) and P – A ($\chi^2(1)=7$; $p=.008$) protocols.
425 Similarly, the M – L direction induced more spread cortical activity than the A – P ($\chi^2(1)=5.8$;
426 $p=.015$) and P – A ($\chi^2(1)=12.5$; $p<.001$) protocols.

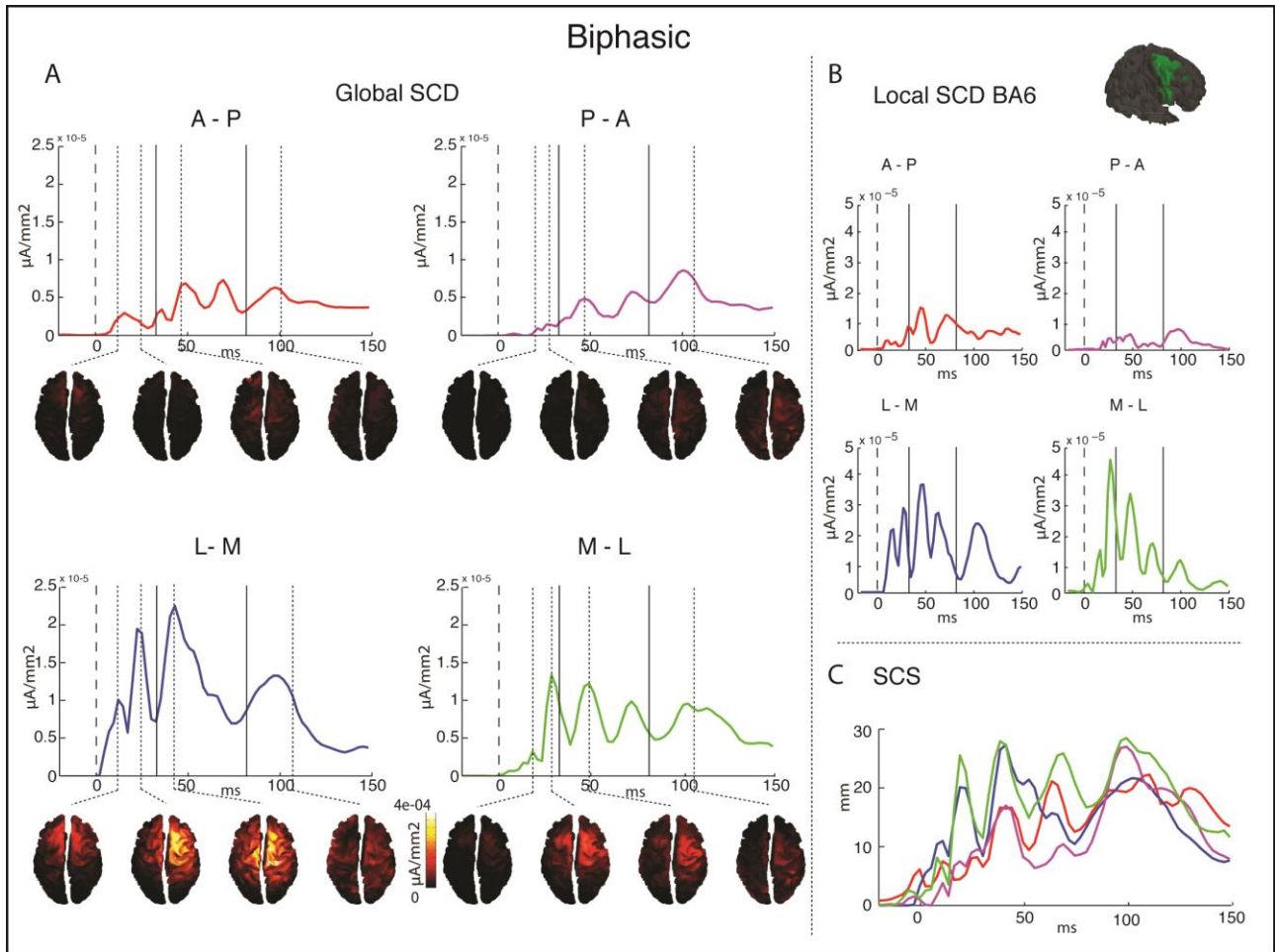
427

428 Time-Frequency analysis

429

430 Time-Frequency analysis showed that L – M biphasic protocol resulted in greater oscillatory activity
431 in the alpha, beta, and high beta bands compared to both A – P (α : $p=.009$; β : $p<.001$; high β : $p<.001$)
432 and P – A (α : $p=.005$; β : $p<.001$; high β : $p<.001$) perpendicular directions. Furthermore, L – M beta
433 activity was higher compared to the other M – L parallel condition ($p=.014$). M – L activity was
434 marginally greater in the high beta band compared to the A – P direction ($p=.057$) (see Fig. 9).

435



436

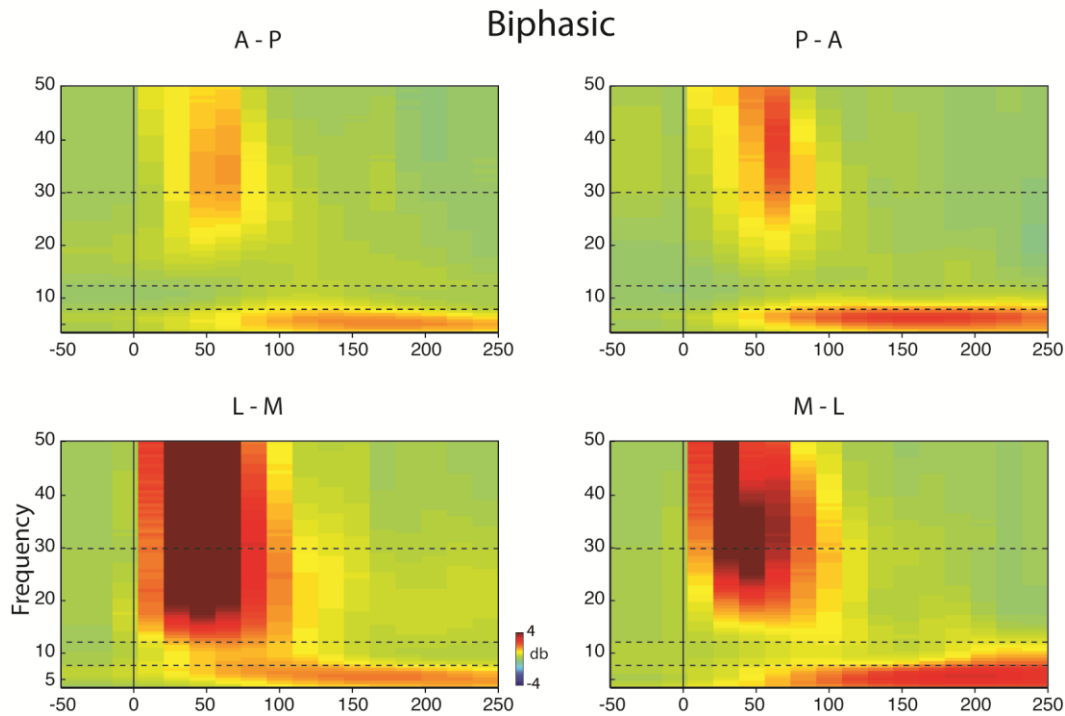
437

438

439

440

Fig. 8: Results of the source analyses for the biphasic protocols. A) plot of the global SCD for the four directions with cortical source reconstruction at the local maxima for each of the three analyzed time windows (0-30ms; 30-80ms; 80-150ms). B) Plot of local SCD in the right BA6. C) plot of the SCS for the 4 protocols.



441

442

443

444

445

446

Discussion

447

448

449

450

451

452

453

454

455

456

457

458

459

460

461

462

Fig 9 Time-frequency representation in the four biphasic directions computed over the four electrodes near the TMS coil (Fz, F2, FCz, FC2). Dashed lines represent the frequency boundaries of the 4 analyzed bands.

In this study, we aimed at exploring possible differences in cortical responses elicited by applying TMS over the premotor cortex with different coil orientations and pulse waveforms. To do so, we measured, using an integrated TMS-EEG system, the cortical response evoked by monophasic and biphasic TMS pulses applied with the TMS coil oriented perpendicular or parallel over the right premotor cortex, following the A – P, P – A, M – L and L – M directions. Overall, TEPs recorded after the biphasic stimulation had greater amplitude than the ones triggered by monophasic pulses. Concerning differences due to coil orientation, an analysis of TEPs time-course showed that this parameter modulated different EEG components, according to which waveform was applied. Biphasic pulses oriented L – M and M – L, i.e., parallel to the stimulated premotor gyrus, evoked a greater early component than A – P or P – A orientations, a difference which was recorded underneath the stimulation site and that was even detectable at parietal sites. Source modelling confirmed this observation, with parallel biphasic stimulation eliciting greater early cortical activity, with more widespread signal scattering, when compared to the perpendicular directions. TEPs spectral features are the typical time-frequency response evoked when stimulating the prefrontal cortex (e.g., Pellicciari et al., 2017; Rosanova et al., 2009), with an early activity peak in the beta and high beta band and a late response in the theta range. Differences in amplitude between the different directions

463 are mirrored by an increase in the power of specific bands. Biphasic TMS applied in the M – L
464 direction induced a diffuse greater activity in the higher frequency bands compared to perpendicular
465 protocols and the other parallel direction.

466 Monophasic pulses, instead, evoked a greater middle-latency component, peaking approximately
467 around 100 ms after TMS onset, over the stimulated area and its contralateral homolog, when oriented
468 A – P or P – A, i.e., perpendicularly to the stimulated gyrus, than when L – M or M – L oriented.
469 Also, in this case, source modeling confirmed greater cortical activity around 100 ms, which spread
470 more over the cortex for the perpendicular compared to the parallel directions. Time-frequency
471 analysis showed a general increase in all frequency bands for the A – P direction compared to the
472 other protocols, and for the P – A compared to the M – L direction.

473 In general, analyses on TEP components amplitude confirmed that biphasic compared to monophasic
474 pulses could elicit greater cortical activity at lower stimulator output levels, in line with previous
475 reports on MEPs. Biphasic pulses, indeed, are more effective compared to monophasic ones in
476 eliciting compound muscle action potentials (CMAPs, Niehaus et al., 2000) for both cortex and nerve
477 stimulation, yielding a lower motor threshold, a shorter MEP latency, a steeper input/output MEP
478 curve (Sommer et al., 2006, 2013; Sommer & Paulus, 2008; Stephani et al., 2016) and having a more
479 complex pattern of cortical activation (Di Lazzaro et al., 2008). This greater cortical activity may be
480 due to the broader stimulation induced by this waveform, which has been supposed to depolarize a
481 greater neural population as compared with monophasic pulses (Arai et al., 2007), especially in its
482 second and third cycle of the waveform (Sommer et al., 2013). Critically, by analyzing the cortical
483 components of the elicited TEPs, we can provide direct evidence of the neurophysiological
484 underpinning of this greater effectiveness of biphasic waveform. In the L - M and M – L stimulation
485 direction, indeed, this type of waveform elicited a greater amplitude in the first TEP components.
486 Early cortical EEG response to TMS has often been associated to several cortical excitability
487 properties of the stimulated area, especially concerning M1 (Mäki & Ilmoniemi, 2010; Ziemann et
488 al., 2015) and prefrontal stimulation (Ilmoniemi & Kičić, 2010). In particular, over the motor cortex
489 three components have usually been reported before 100ms post TMS, peaking around 30, 45 and
490 60ms (Ziemann et al., 2015), and similar components have been described for the premotor cortex,
491 even if some differences in amplitude and latency are present (Casarotto et al., 2010; Lioumis et al.,
492 2009). The neurophysiological mechanisms generating these components have been debated in the
493 literature. Early TEP components were modulated by tDCS when measured both from M1 (Pellicciari
494 et al., 2013) and the prefrontal cortex (Pisoni et al., 2017), clearly building a bridge between the
495 amplitude of these components and cortical excitability of the stimulated area. Similarly, Komssi et
496 al. (2004) showed that these components are the most influenced by TMS intensity. Pharmacological

497 research, instead, showed that GABA_A receptors inhibition modulates an early component peaking at
498 45ms (Premoli et al., 2014). It has to be noted, however, that while this modulation in cortical
499 inhibition showed a topography centered over the cortical regions contralateral to the TMS target
500 (Premoli et al., 2014), modulation of cortical excitability effects remained under the stimulated area
501 (Pellicciari et al., 2013; Source reconstruction in Pisoni et al., 2017). Thus, it is possible that these
502 early components reflect different neurophysiological processes, which are related to intracortical
503 inhibition (in regions connected to the target area) and cortical excitability of the stimulated cortical
504 site. The present results show an increase in the early TEP components with the L-M biphasic
505 waveform orientation which is centered over the stimulated region, supporting the hypothesis that
506 this protocol is the most efficient in triggering action potential from pyramidal neurons directly under
507 the stimulator, rather than a cortico-cortical response (Ilmoniemi & Kičić, 2010). In line with this,
508 MEP research reported that L - M currents had been shown to induce D-waves, which are a reflection
509 of direct layer V pyramidal neurons depolarization, even at low intensities (Di Lazzaro et al., 1998;
510 for a review see Di Lazzaro et al., 2008; Di Lazzaro & Ziemann, 2013). A recruitment of this neural
511 population might end in a greater TEP first component.

512 Conversely, for the monophasic pulse, the A - P and P - A directions, which run perpendicular to the
513 targeted gyrus, were more efficient than the L-M orientation to elicit a 100 ms latency component.
514 This component is one of the most commonly reported and more reproducible TEP component in
515 literature (Bender et al., 2005; Bonnard et al., 2009; Kähkönen & Wilenius, 2007; Kičić, 2009;
516 Lioumis et al., 2009; Massimini et al., 2005; Nikulin et al., 2003; Paus et al., 2001), and has been
517 consistently associated with cortico-cortical inhibitory activity (Bikmullina et al., 2009; Premoli et
518 al., 2014; for a review see Ilmoniemi & Kičić, 2010). Specifically, N100 amplitude has been found
519 to be negatively associated with MEP amplitude (Kičić et al., 2008), it is modulated by coil orientation
520 (Bonato et al., 2006) and linked with short intra-cortical inhibition (SICI) and with long intra-cortical
521 inhibition (LICI) induced by paired-pulse TMS (Daskalakis et al., 2008; Ferreri et al., 2011;
522 Fitzgerald et al., 2009; Rogasch & Fitzgerald, 2013). Moreover, if M1 is active while measuring TEPs
523 or is prepared to perform an action, N100 results reduced (Bender et al., 2005; Nikulin et al., 2003),
524 but increased when the action is inhibited (Bonnard et al., 2009). Similarly, studies applying theta
525 burst stimulation on the prefrontal cortex showed a modulation of the 100ms component which was
526 linked to markers of cortical inhibition as LICI (Chung et al., 2017). Pharmacological studies finally
527 proved the link between GABA_B receptors and N100 amplitude, showing that the administration of
528 baclofen, a GABA_B receptor agonist, significantly enhanced N100 amplitude (Premoli et al., 2014).
529 Crucially, Premoli and colleagues (2014), showed that the intracortical inhibitory component linked
530 to GABA_B receptors showed a topography encompassing cortical areas contralateral to the TMS

531 target. Similarly, we highlighted an increase in the 100ms component, which shows a scalp
532 distribution including the stimulation site and its contralateral counterpart, suggesting greater
533 recruitment of trans-callosal inhibitory connections running between homolog regions of the two
534 hemispheres. Monophasic pulse perpendicularly applied with respect to the stimulated cortical gyrus,
535 thus, seem to be the best-suited protocols to highlight, and possibly modulate, neurophysiological
536 processes relying on such connections. In this sense, our data fit well with rTMS findings which
537 report monophasic pulses as being more efficient in inducing inhibitory after-effects following low-
538 frequency rTMS protocols (Sommer et al., 2002; Taylor & Loo, 2007), especially with the A - P pulse
539 direction (Tings et al., 2005).

540 Finally, it has to be noted that by using the TMS-EEG approach we were able to reveal
541 neurophysiological differences in stimulation protocols which up to now were derived from indirect
542 measures of cortical response, such as MEP or spinal recordings and limited to M1 or V1 stimulation.
543 This opens a whole new scenario in which effects of different stimulation protocols can be directly
544 tested by applying TMS over the target cortical region of interest.

545 As a potential limitation, we have to point out that monophasic and biphasic stimulation elicit
546 different auditory and somatosensory feelings. Even if we did not directly compare the two pulses,
547 and applied efficient masking techniques (Ter Braak et al., 2015), we cannot exclude some influence
548 of these effects on our results. However, as Ter Braak and collaborators (2015) demonstrated, both
549 auditory and bone conduction-related feelings do not affect early TEP components, while they do
550 affect the N100 complex. However, since we had a modulation of this component by tilting the
551 monophasic pulse, while no modulation occurred with the biphasic stimulation, we feel like it is
552 unlikely that haptic sensations are involved in this effect.

553 From a theoretical point of view, our results support with direct evidence the hypothesis that different
554 pulse waveforms and directions do have different stimulation outcomes in terms of targeted neural
555 population and induced cortical mechanisms: results showed that biphasic pulse oriented parallel to
556 the stimulated premotor gyrus triggered cortical excitability mechanisms within the target area, while
557 monophasic stimulation perpendicularly oriented to the target gyrus mainly triggered inhibitory
558 interneurons. These findings may guide scientists and clinicians using TMS as their research and
559 treatment method in designing more efficient stimulation protocols to address their scientific goals.

560

561 References

562

- 563 1. Antal, A., Kincses, T. Z., Nitsche, M. A., Bartfai, O., Demmer, I., Sommer, M., & Paulus, W.
564 (2002). Pulse configuration-dependent effects of repetitive transcranial magnetic stimulation
565 on visual perception. *Neuroreport*, 13(17), 2229-2223.
- 566 2. Arai, N., Okabe, S., Furubayashi, T., Mochizuki, H., Iwata, N. K., Hanajima, R., ... & Ugawa,
567 Y. (2007). Differences in after-effect between monophasic and biphasic high-frequency rTMS
568 of the human motor cortex. *Clinical Neurophysiology*, 118(10), 2227-2233.
- 569 3. Arai, N., Okabe, S., Furubayashi, T., Terao, Y., Yuasa, K., & Ugawa, Y. (2005). Comparison
570 between short train, monophasic and biphasic repetitive transcranial magnetic stimulation
571 (rTMS) of the human motor cortex. *Clinical Neurophysiology*, 116(3), 605-613.
- 572 4. Ashburner, J., Barnes, G., Chen, C. C., Daunizeau, J., Flandin, G., & Friston, K. (2011).
573 SPM8. *Functional Imaging Laboratory, Institute of Neurology*, 12.
- 574 5. Baayen, R. H., Davidson, D. J., & Bates, D. M. (2008). Mixed-effects modeling with crossed
575 random effects for subjects and items. *Journal of memory and language*, 59(4), 390-412.
- 576 6. Bender, S., Basseler, K., Sebastian, I., Resch, F., Kammer, T., Oelkers-Ax, R., & Weisbrod,
577 M. (2005). Transcranial magnetic stimulation evokes giant inhibitory potentials in children.
578 *Annals of neurology*, 58(1), 58.
- 579 7. Bikmullina, R., Kičić, D., Carlson, S., & Nikulin, V. V. (2009). Electrophysiological
580 correlates of short-latency afferent inhibition: a combined EEG and TMS study. *Experimental*
581 *brain research*, 194(4), 517-526.
- 582 8. Bonato, C., Miniussi, C., & Rossini, P. M. (2006). Transcranial magnetic stimulation and
583 cortical evoked potentials: a TMS/EEG co-registration study. *Clinical neurophysiology*,
584 117(8), 1699-1707.
- 585 9. Bonnard, M., Spieser, L., Meziane, H. B., De Graaf, J. B., & Pailhous, J. (2009). Prior
586 intention can locally tune inhibitory processes in the primary motor cortex: direct evidence
587 from combined TMS-EEG. *European Journal of Neuroscience*, 30(5), 913-923.
- 588 10. Casali, A. G., Casarotto, S., Rosanova, M., Mariotti, M., & Massimini, M. (2010). General
589 indices to characterize the electrical response of the cerebral cortex to TMS. *Neuroimage*,
590 49(2), 1459-1468.
- 591 11. Casali, A. G., Gosseries, O., Rosanova, M., Boly, M., Sarasso, S., Casali, K. R., ... &
592 Massimini, M. (2013). A theoretically based index of consciousness independent of sensory
593 processing and behaviour. *Science translational medicine*, 5(198), 198ra105-198ra105.

- 594 12. Casarotto, S., Lauro, L. J. R., Bellina, V., Casali, A. G., Rosanova, M., Pigorini, A., ... &
595 Massimini, M. (2010). EEG responses to TMS are sensitive to changes in the perturbation
596 parameters and repeatable over time. *PLoS One*, 5(4), e10281.
- 597 13. Chung, S. W., Lewis, B. P., Rogasch, N. C., Saeki, T., Thomson, R. H., Hoy, K. E., ... &
598 Fitzgerald, P. B. (2017). Demonstration of short-term plasticity in the dorsolateral prefrontal
599 cortex with theta burst stimulation: A TMS-EEG study. *Clinical Neurophysiology*.
- 600 14. Daskalakis, Z. J., Farzan, F., Barr, M. S., Maller, J. J., Chen, R., & Fitzgerald, P. B. (2008).
601 Long-interval cortical inhibition from the dorsolateral prefrontal cortex: a TMS-EEG study.
602 *Neuropsychopharmacology*, 33(12), 2860-2869.
- 603 15. Delorme, A., & Makeig, S. (2004). EEGLAB: an open source toolbox for analysis of single-
604 trial EEG dynamics including independent component analysis. *Journal of neuroscience*
605 *methods*, 134(1), 9-21.
- 606 16. Delorme, A., Sejnowski, T., & Makeig, S. (2007). Enhanced detection of artifacts in EEG
607 data using higher-order statistics and independent component analysis. *Neuroimage*, 34(4),
608 1443-1449.
- 609 17. Di Lazzaro, V., Restuccia, D., Oliviero, A., Profice, P., Ferrara, L., Insola, A., ... & Rothwell,
610 J. C. (1998). Effects of voluntary contraction on descending volleys evoked by transcranial
611 stimulation in conscious humans. *The Journal of physiology*, 508(2), 625-633
- 612 18. Di Lazzaro, V., Ziemann, U., & Lemon, R. N. (2008). State of the art: physiology of
613 transcranial motor cortex stimulation. *Brain Stimulation*, 1: 345-62.
- 614 19. Di Lazzaro, V., & Ziemann, U. (2013). The contribution of transcranial magnetic stimulation
615 in the functional evaluation of microcircuits in human motor cortex. *Frontiers in neural*
616 *circuits*, 7: 18.
- 617 20. Esser, S. K., Huber, R., Massimini, M., Peterson, M. J., Ferrarelli, F., & Tononi, G. (2006).
618 A direct demonstration of cortical LTP in humans: a combined TMS/EEG study. *Brain*
619 *research bulletin*, 69(1), 86-94.
- 620 21. Ferreri, F., Pasqualetti, P., Määttä, S., Ponzio, D., Ferrarelli, F., Tononi, G., ... & Rossini, P.
621 M. (2011). Human brain connectivity during single and paired pulse transcranial magnetic
622 stimulation. *Neuroimage*, 54(1), 90-102.
- 623 22. Fitzgerald, P. B., Maller, J. J., Hoy, K., Farzan, F., & Daskalakis, Z. J. (2009). GABA and
624 cortical inhibition in motor and non-motor regions using combined TMS-EEG: A time
625 analysis. *Clinical neurophysiology*, 120(9), 1706-1710.

- 626 23. Groppa, S., Oliviero, A., Eisen, A., Quartarone, A., Cohen, L. G., Mall, V., ... & Rossini, P.
627 M. (2012). A practical guide to diagnostic transcranial magnetic stimulation: report of an
628 IFCN committee. *Clinical Neurophysiology*, 123(5), 858-882.
- 629 24. Hämäläinen, M. S., & Ilmoniemi, R. J. (1994). Interpreting magnetic fields of the brain:
630 minimum norm estimates. *Medical & biological engineering & computing*, 32(1), 35-42.
- 631 25. Ilmoniemi, R. J., & Kičić, D. (2010). Methodology for combined TMS and EEG. *Brain*
632 *topography*, 22(4), 233-248.
- 633 26. Ilmoniemi, R. J., Virtanen, J., Ruohonen, J., Karhu, J., Aronen, H. J., & Katila, T. (1997).
634 Neuronal responses to magnetic stimulation reveal cortical reactivity and connectivity.
635 *Neuroreport*, 8(16), 3537-3540.
- 636 27. Julkunen, P., Pääkkönen, A., Hukkanen, T., Könönen, M., Tiihonen, P., Vanhatalo, S., &
637 Karhu, J. (2008). Efficient reduction of stimulus artefact in TMS-EEG by epithelial short-
638 circuiting by mini-punctures. *Clinical Neurophysiology*, 119(2), 475-481.
- 639 28. Kähkönen, S., & Wilenius, J. (2007). Effects of alcohol on TMS-evoked N100 responses.
640 *Journal of neuroscience methods*, 166(1), 104-108.
- 641 29. Kähkönen, S., Komssi, S., Wilenius, J., & Ilmoniemi, R. J. (2005). Prefrontal TMS produces
642 smaller EEG responses than motor-cortex TMS: implications for rTMS treatment in
643 depression. *Psychopharmacology*, 181(1), 16-20.
- 644 30. Kammer, T., Beck, S., Thielscher, A., Laubis-Herrmann, U., & Topka, H. (2001). Motor
645 thresholds in humans: a transcranial magnetic stimulation study comparing different pulse
646 waveforms, current directions and stimulator types. *Clinical neurophysiology*, 112(2), 250-
647 258.
- 648 31. Keel, J. C., Smith, M. J., & Wassermann, E. M. (2001). A safety screening questionnaire for
649 transcranial magnetic stimulation. *Clinical neurophysiology*, 112(4), 720.
- 650 32. Kičić, D., Lioumis, P., Ilmoniemi, R. J., & Nikulin, V. V. (2008). Bilateral changes in
651 excitability of sensorimotor cortices during unilateral movement: combined
652 electroencephalographic and transcranial magnetic stimulation study. *Neuroscience*, 152(4),
653 1119-1129.
- 654 33. Kičić, D. (2009). Probing cortical excitability with transcranial magnetic stimulation.
655 *University of Technology*.
- 656 34. Komssi, S., Aronen, H. J., Huttunen, J., Kesäniemi, M., Soinne, L., Nikouline, V. V., ... &
657 Ilmoniemi, R. J. (2002). Ipsi-and contralateral EEG reactions to transcranial magnetic
658 stimulation. *Clinical Neurophysiology*, 113(2), 175-184.

- 659 35. Komssi, S., Kähkönen, S., & Ilmoniemi, R. J. (2004). The effect of stimulus intensity on brain
660 responses evoked by transcranial magnetic stimulation. *Human brain mapping*, 21(3), 154-
661 164.
- 662 36. Komssi, S., Savolainen, P., Heiskala, J., & Kähkönen, S. (2007). Excitation threshold of the
663 motor cortex estimated with transcranial magnetic stimulation electroencephalography.
664 *Neuroreport*, 18(1), 13-16.
- 665 37. Lefaucheur, J. P., André-Obadia, N., Antal, A., Ayache, S. S., Baeken, C., Benninger, D. H.,
666 ... & Devanne, H. (2014). Evidence-based guidelines on the therapeutic use of repetitive
667 transcranial magnetic stimulation (rTMS). *Clinical Neurophysiology*, 125(11), 2150-2206.
- 668 38. Lioumis, P., Kičić, D., Savolainen, P., Mäkelä, J. P., & Kähkönen, S. (2009). Reproducibility
669 of TMS—Evoked EEG responses. *Human brain mapping*, 30(4), 1387-1396.
- 670 39. Litvak, V., Mattout, J., Kiebel, S., Phillips, C., Henson, R., Kilner, J., ... & Penny, W. (2011).
671 EEG and MEG data analysis in SPM8. *Computational intelligence and neuroscience*, 2011.
- 672 40. Luber, B., & Lisanby, S. H. (2014). Enhancement of human cognitive performance using
673 transcranial magnetic stimulation (TMS). *Neuroimage*, 85, 961-970.
- 674 41. Maccabee, P. J., Nagarajan, S. S., Amassian, V. E., Durand, D. M., Szabo, A. Z., Ahad, A.
675 B., ... & Eberle, L. P. (1998). Influence of pulse sequence, polarity and amplitude on magnetic
676 stimulation of human and porcine peripheral nerve. *The Journal of physiology*, 513(2), 571-
677 585.
- 678 42. Mäki, H., & Ilmoniemi, R. J. (2010). EEG oscillations and magnetically evoked motor
679 potentials reflect motor system excitability in overlapping neuronal populations. *Clinical*
680 *Neurophysiology*, 121(4), 492-501.
- 681 43. Maris, E., & Oostenveld, R. (2007). Nonparametric statistical testing of EEG-and MEG-data.
682 *Journal of neuroscience methods*, 164(1), 177-190.
- 683 44. Massimini, M., Ferrarelli, F., Huber, R., Esser, S. K., Singh, H., & Tononi, G. (2005).
684 Breakdown of cortical effective connectivity during sleep. *Science*, 309(5744), 2228-2232.
- 685 45. Mattavelli, G., Rosanova, M., Casali, A. G., Papagno, C., & Lauro, L. J. R. (2016). Timing of
686 emotion representation in right and left occipital region: Evidence from combined TMS-EEG.
687 *Brain and Cognition*, 106, 13-22.
- 688 46. Mattavelli, G., Rosanova, M., Casali, A. G., Papagno, C., & Lauro, L. J. R. (2013). Top-down
689 interference and cortical responsiveness in face processing: a TMS-EEG study. *Neuroimage*,
690 76, 24-32.
- 691 47. Mütanen, T., Mäki, H., & Ilmoniemi, R. J. (2013). The effect of stimulus parameters on TMS—
692 EEG muscle artefacts. *Brain stimulation*, 6(3), 371-376.

- 693 48. Niehaus, L., Meyer, B. U., & Weyh, T. (2000). Influence of pulse configuration and direction
694 of coil current on excitatory effects of magnetic motor cortex and nerve stimulation. *Clinical*
695 *Neurophysiology*, 111(1), 75-80.
- 696 49. Nikulin, V. V., Kičić, D., Kähkönen, S., & Ilmoniemi, R. J. (2003). Modulation of
697 electroencephalographic responses to transcranial magnetic stimulation: evidence for changes
698 in cortical excitability related to movement. *European Journal of Neuroscience*, 18(5), 1206-
699 1212.
- 700 50. Oostenveld, R., Fries, P., Maris, E., & Schoffelen, J. M. (2011). FieldTrip: open source
701 software for advanced analysis of MEG, EEG, and invasive electrophysiological
702 data. *Computational intelligence and neuroscience*, 2011, 1.
- 703 51. Pantazis, D., Nichols, T. E., Baillet, S., & Leahy, R. M. (2003, July). Spatiotemporal
704 localization of significant activation in MEG using permutation tests. In *Biennial*
705 *International Conference on Information Processing in Medical Imaging* (pp. 512-523).
706 Springer, Berlin, Heidelberg.
- 707 52. Paus, T., Sipila, P. K., & Strafella, A. P. (2001). Synchronization of neuronal activity in the
708 human primary motor cortex by transcranial magnetic stimulation: an EEG study. *Journal of*
709 *Neurophysiology*, 86(4), 1983-1990.
- 710 53. Pascual-Leone, A., Valls-Solé, J., Wassermann, E. M., & Hallett, M. (1994). Responses to
711 rapid-rate transcranial magnetic stimulation of the human motor cortex. *Brain*, 117(4), 847-
712 858.
- 713 54. Pellicciari, M. C., Brignani, D., & Miniussi, C. (2013). Excitability modulation of the motor
714 system induced by transcranial direct current stimulation: a multimodal approach.
715 *Neuroimage*, 83, 569-580.
- 716 55. Pellicciari, M. C., Ponzio, V., Caltagirone, C., & Koch, G. (2017). Restored asymmetry of
717 prefrontal cortical oscillatory activity after bilateral theta burst stimulation treatment in a
718 patient with major depressive disorder: a TMS-EEG study. *Brain Stimulation: Basic,*
719 *Translational, and Clinical Research in Neuromodulation*, 10(1), 147-149.
- 720 56. Peterchev, A. V., Wagner, T. A., Miranda, P. C., Nitsche, M. A., Paulus, W., Lisanby, S. H.,
721 ... & Bikson, M. (2012). Fundamentals of transcranial electric and magnetic stimulation dose:
722 definition, selection, and reporting practices. *Brain Stimulation: Basic, Translational, and*
723 *Clinical Research in Neuromodulation*, 5(4), 435-453.
- 724 57. Pisoni, A., Mattavelli, G., Papagno, C., Rosanova, M., Casali, A. G., & Romero Lauro, L. J.
725 (2017). Cognitive Enhancement Induced by Anodal tDCS Drives Circuit-Specific Cortical
726 Plasticity. *Cerebral Cortex*, 1-9.

- 727 58. Premoli, I., Castellanos, N., Rivolta, D., Belardinelli, P., Bajo, R., Zipser, C., ... & Ziemann,
728 U. (2014). TMS-EEG signatures of GABAergic neurotransmission in the human cortex. *The*
729 *Journal of Neuroscience*, 34(16), 5603-5612.
- 730 59. R Development Core Team, 2008. R: a language and environment for statistical computing,
731 60. Vienna, Austria R Foundation for Statistical Computing Available at ([http://www.R-](http://www.R-project.org)
732 [project.org](http://www.R-project.org)).
- 733 61. Rogasch, N. C., & Fitzgerald, P. B. (2013). Assessing cortical network properties using TMS–
734 EEG. *Human brain mapping*, 34(7), 1652-1669.
- 735 62. Romero Lauro, L. J. R., Pisoni, A., Rosanova, M., Casarotto, S., Mattavelli, G., Bolognini,
736 N., & Vallar, G. (2016). Localizing the effects of anodal tDCS at the level of cortical sources:
737 A Reply to Bailey et al., 2015. *Cortex*, (74), 323-328.
- 738 63. Romero Lauro, L. J. R., Rosanova, M., Mattavelli, G., Convento, S., Pisoni, A., Opitz, A., ...
739 & Vallar, G. (2014). TDCS increases cortical excitability: Direct evidence from TMS–EEG.
740 *Cortex*, 58, 99-111.
- 741 64. Rosanova, M., Casali, A., Bellina, V., Resta, F., Mariotti, M., & Massimini, M. (2009).
742 Natural frequencies of human corticothalamic circuits. *Journal of Neuroscience*, 29(24),
743 7679-7685.
- 744 65. Rossi, S., Hallett, M., Rossini, P. M., Pascual-Leone, A., & Safety of TMS Consensus Group.
745 (2009). Safety, ethical considerations, and application guidelines for the use of transcranial
746 magnetic stimulation in clinical practice and research. *Clinical neurophysiology*, 120(12),
747 2008-2039.
- 748 66. Silva, C., Maltez, J. C., Trindade, E., Arriaga, A., & Ducla-Soares, E. (2004). Evaluation of
749 L1 and L2 minimum norm performances on EEG localizations. *Clinical neurophysiology*,
750 115(7), 1657-1668.
- 751 67. Sommer, M., Alfaro, A., Rummel, M., Speck, S., Lang, N., Tings, T., & Paulus, W. (2006).
752 Half sine, monophasic and biphasic transcranial magnetic stimulation of the human motor
753 cortex. *Clinical Neurophysiology*, 117(4), 838-844.
- 754 68. Sommer, M., Lang, N., Tergau, F., & Paulus, W. (2002). Neuronal tissue polarization induced
755 by repetitive transcranial magnetic stimulation?. *Neuroreport*, 13(6), 809-811.
- 756 69. Sommer, M., Norden, C., Schmack, L., Rothkegel, H., Lang, N., & Paulus, W. (2013).
757 Opposite optimal current flow directions for induction of neuroplasticity and excitation
758 threshold in the human motor cortex. *Brain stimulation*, 6(3), 363-370.

- 759 70. Sommer, M., & Paulus, W. (2008). TMS waveform and current direction. In “The Oxford
760 handbook of transcranial stimulation”, Epstein, C.M., Wasserman, E.M. and Ziemann, U.
761 Oxford University Press, New York, 7-12.
- 762 71. Sparing, R., Hesse, M. D., & Fink, G. R. (2010). Neuronavigation for transcranial magnetic
763 stimulation (TMS): where we are and where we are going. *Cortex*, 46(1), 118-120.
- 764 72. Stephani, C., Paulus, W., & Sommer, M. (2016). The effect of current flow direction on motor
765 hot spot allocation by transcranial magnetic stimulation. *Physiological reports*, 4(1), e12666.
- 766 73. Taylor, J. L., & Loo, C. K. (2007). Stimulus waveform influences the efficacy of repetitive
767 transcranial magnetic stimulation. *Journal of affective disorders*, 97(1), 271-276.
- 768 74. Ter Braack, E. M., de Vos, C. C., & van Putten, M. J. (2015). Masking the auditory evoked
769 potential in TMS–EEG: A comparison of various methods. *Brain topography*, 28(3), 520-
770 528.
- 771 75. Tings, T., Lang, N., Tergau, F., Paulus, W., & Sommer, M. (2005). Orientation-specific fast
772 rTMS maximizes corticospinal inhibition and facilitation. *Experimental brain research*,
773 164(3), 323-333.
- 774 76. Triesch, J., Zrenner, C., & Ziemann, U. (2015). Modeling TMS-induced I-waves in human
775 motor cortex. *Progress in brain research*, 222, 105-124.
- 776 77. Veniero, D., Bortoletto, M., & Miniussi, C. (2012). Cortical modulation of short-latency
777 TMS-evoked potentials. *Frontiers in human neuroscience*, 6.
- 778 78. Veniero, D., Maioli, C., & Miniussi, C. (2010). Potentiation of short-latency cortical
779 responses by high-frequency repetitive transcranial magnetic stimulation. *Journal of*
780 *neurophysiology*, 104(3), 1578-1588.
- 781 79. Virtanen, J., Ruohonen, J., Nääätänen, R., & Ilmoniemi, R. J. (1999). Instrumentation for the
782 measurement of electric brain responses to transcranial magnetic stimulation. *Medical &*
783 *biological engineering & computing*, 37(3), 322-326.
- 784 80. Zanon, M., Battaglini, P. P., Jarmolowska, J., Pizzolato, G., & Busan, P. (2013). Long-range
785 neural activity evoked by premotor cortex stimulation: a TMS/EEG co-registration study.
786 *Frontiers in human neuroscience*, 7, 803.
- 787 81. Ziemann, U., Reis, J., Schwenkreis, P., Rosanova, M., Strafella, A., Badawy, R., & Müller-
788 Dahlhaus, F. (2015). TMS and drugs revisited 2014. *Clinical neurophysiology*, 126(10),
789 1847-1868.